Article

# Conformational Properties of Shape Modified Nucleosides – Fleximers

Matja Polak, Katherine L. Seley, and Janez Plavec

*J. Am. Chem. Soc.*, **2004**, 126 (26), 8159-8166• DOI: 10.1021/ja0498078 • Publication Date (Web): 12 June 2004



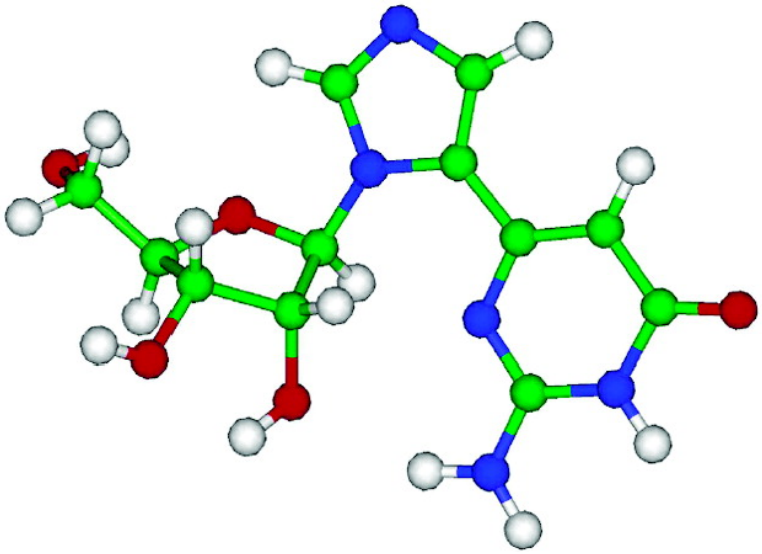

J|A|C|S
ARTICLES
Published on Web 06/12/2004

# Conformational Properties of Shape Modified Nucleosides − Fleximers

Matjaž Polak,[†] Katherine L. Seley,[‡] and Janez Plavec*,[†]

*Contribution from the Slovenian NMR Center, National Institute of Chemistry, Hajdrihova 19, POB 660, SI-1001 Ljubljana, Slovenia, and Department of Chemistry and Biochemistry, University of Maryland, Baltimore County, Baltimore, Maryland, 21250*

Received January 12, 2004; E-mail: janez.plavec@ki.si

***Abstract:*** A detailed $^1$H NMR conformational study complemented with ab initio computations was performed in solution on fleximer nucleosides **1**, **3**, and **5** in relation to their natural counterparts. The substitution of the purine nucleobase found in the natural nucleosides with a more flexible two-ring heterocyclic system strongly increased the population of anti conformation around the glycosidic bond. This was accompanied by a large shift toward a north-type sugar conformation, which was explained by the interplay of anomeric, gauche, and steric effects. The formal separation of the bicyclic purine base into its imidazole and pyrimidine moieties allows for formation of a hydrogen bond between the $NH_2$ and 2′-OH groups and facilitates favorable conjugation between the two heterocyclic rings. Our results show that the interplay of stereoelectronic effects, combined with the flexibility of the nucleobase and possible conjugation effects within the nucleobase, plays a crucial role in the search for shape-mimic nucleosides that will interact with flexible binding sites.

## Introduction

Chemical modification of nucleosides and their incorporation into nucleic acid oligomers represent one of the most successful drug design strategies when considering chemotherapeutic approaches, as is evidenced by the significant number of analogues in clinical trials for treatment of various diseases including cancer, inflammation, and viral infections.[1] Numerous modifications to the sugar ring as well as the heterocyclic nucleobase moieties have been utilized in recent years to increase chemotherapeutic activity.[2,3] A new class of shape-modified nucleosides called fleximers has recently been introduced.[4] The purine nucleobase of the fleximers is split into its imidazole and pyrimidine components, which remain connected by a single C−C bond. This allows the modified nucleosides to more readily adopt to the spatial and other requirements of the binding site, while at the same time retaining the majority of the key structural features required for molecular recognition. The guanosine fleximer **5** has been shown to inhibit *S*-adenosyl-L-homocysteine hydrolase (SAHase).[5] This finding was intriguing because there have been no other reports of a guanosine analogue inhibiting this biologically significant adenosine-metabolizing enzyme. As anticipated, however, no inhibitory activity was observed for the adenosine fleximer **3** which instead served as a substrate for SAHase.[5] On the basis of ab initio calculations that were carried out on the guanosine fleximer **5**, it was suggested that one possible explanation of the unusual inhibitory activity could be attributed to the ability of the nucleobase to adopt an unusual syn conformation when interacting with the flexible binding site of SAHase.[5] A combined NMR and ab initio conformational study on the inosine (**1**), adenosine (**3**), and guanosine fleximers (**5**) in solution was then initiated in order to assess the possibility of additional conformational degrees of freedom within the heterocyclic aglycon. In addition, possible interdependence with standard conformational equilibria of the north and south puckered forms of ribofuranosyl moieties as well as along glycosidic and C4′−C5′ bonds was explored. Conformational properties of fleximer nucleosides **1**, **3**, and **5** were compared with their natural counterparts to gain insight as to the importance of structural and stereoelectronic properties and integrity of heterocyclic nucleobases as well as their importance in influencing the tunability of the sugar−phosphate backbone conformation above and beyond the normal recognition and molecular assembly through hydrogen bonds.

The pentofuranose sugar moiety in nucleosides is intrinsically involved in dynamic north (N, roughly C3′-*endo*) ⇄ south (S, roughly C2′-*endo*) pseudorotational equilibrium between different puckering modes. Numerous analyses of a two-state N ⇄ S pseudorotational equilibrium in nucleosides and nucleotides have shown that the preferred sugar conformation is controlled by the gauche effects of [O4′-C−C−O3′/2′] fragments, the anomeric effect of the heterocyclic nucleobase, and steric interactions.[6−9] In this case, the formal separation of the purine nucleobase into its separate imidazole and pyrimidine compo-

[†] National Institute of Chemistry.
[‡] University of Maryland, Baltimore County.

(1) Papers presented at XV International Roundtable Nucleosides, Nucleotides and Nucleic Acids, Leuven, Belgium, September 2002. *Nucleosides Nucleotides Nucl. Acids.* **2003**, *22*, 489−1736.
(2) Agrawal, S.; Zhao, Q. Y. *Curr. Opin. Chem. Biol.* **1998**, *2*, 519−528.
(3) De Clercq, E. *Clin. Microbiol. Rev.* **2003**, *16*, 569−596.
(4) Seley, K. L.; Zhang, L.; Hagos, A.; Quirk, S. *J. Org. Chem.* **2002**, *67*, 3365−3373.
(5) Seley, K. L.; Quirk, S.; Salim, S.; Zhang, L.; Hagos, A. *Bioorg. Med. Chem. Lett.* **2003**, *13*, 1985−1988.
(6) Plavec, J.; Tong, W. M.; Chattopadhyaya, J. *J. Am. Chem. Soc.* **1993**, *115*, 9734−9746.

10.1021/ja0498078 CCC: $27.50 

nents endows the fleximer with even more conformational heterogeneity, therefore making it possible to adapt more readily to the spatial confines of potential binding sites. The study presented herein was initiated to gain a better understanding as to whether greater flexibility for nucleoside analogues is correlated with the intrinsic stereoelectronic factors that govern the conformation of sugar−phosphate backbone in nucleosides and nucleotides in general. Insights into the complex relationships of conformational properties and the potential for biological activity are of great importance in understanding the structural makeup and, consequently, the various functional roles of the nucleic acids.

## Materials and Methods

**NMR Measurements.** $^1$H NMR spectra were recorded on Varian Unity Inova 300 NMR spectrometer at the Slovenian NMR center at 297.8 MHz. Spectra were acquired at 10 mM concentration of **1**−**6** in DMSO-$d_6$ (99.9% deuterium) and with their saturated solutions in $D_2O$ (99.96% deuterium) at concentrations below 1 mM for **1**, **3**, and **5**. All proton resonances of sugar and nucleobase protons were completely assigned with the use of 1D $^1$H homonuclear decoupling, $T_1$ relaxation time measurements, and 1D NOE experiments. $^3J_{HH}$ coupling constants and populations along C4′−C5′ bonds for **6** in DMSO-$d_6$[10] and data for **4** and **6** in $D_2O$[11] were taken from our previous work. Tetramethylsilane (TMS) in DMSO-$d_6$ and sodium trimethylsilyl propionate (TMSP) were used as internal reference ($\delta = 0.000$ ppm) for $^1$H NMR spectra. Error in determination of coupling constants was ±0.1 Hz for $J_{HH}$. The sample temperature was varied from 298 to 358 K and controlled to approximately ±0.1 K.

1D $^1$H measurements were performed under the following spectral and processing conditions: 5.4 kHz sweep width, 32K time domain, zero filling to 128K, and slight Gaussian apodization to give enhanced resolution. 1D NOE experiments were run with saturation of individual lines within the multiplets and by internal subtraction of on- and off-resonance spectra. 1D NOE experiments were acquired with a 50 ms mixing time.

**Conformational Analysis.** Conformational analysis of the sugar moieties was performed with the computer program PSEUROT with the use of $\lambda$ electronegativities for the substituents along H−C−C−H fragments and the six-parameter generalized Karplus−Altona equation.[12,13] Substituent $\lambda$ electronegativities were obtained through the iterative procedure[13] that gave the best fit between experimentally measured $^3J_{HH}$ coupling constants and respective torsion angles in a large set of compounds and reflect the nature of a particular substituent. The following $\lambda$ electronegativity values were used: 0.0 for H; 0.58 for the heterocyclic base; 1.26 for OH; 0.62 for C1′, C2′, C3′, and C4′; 1.27 for O4′; and 0.68 for C5′.[13] In the optimization procedure, both geometries and populations of N- and S-type pseudorotamers were varied to obtain the best fit between the experimental and calculated coupling constants. Our optimization procedure started with the following values: $P_N = 18°$, $\Psi_m{}^N = 36°$, $P_S = 162°$, and $\Psi_m{}^S = 36°$. The phase angle of pseudorotation and puckering amplitude of the minor S-type conformer were kept frozen during the individual iterative least-squares optimization, whereas parameters for the major N-type conformer were freely optimized and vice versa. The optimization resulted in the following ranges of P and $\Psi_m$ for the N- and S-type geometries in all residues which best agreed with the experimental $^3J_{HH}$ coupling constant data: $-8° < P_N < 41°$, $128° < P_S < 178°$, $31° < \Psi_m{}^N = \Psi_m{}^S < 35°$, rms < 0.15 Hz, $\Delta J_{max} < 0.24$ Hz for individual residues in flexrI (**1**); $-25° < P_N < 28°$, $134° < P_S < 153°$, $30° < \Psi_m{}^N = \Psi_m{}^S < 36°$, rms < 0.10 Hz, $\Delta J_{max} < 0.23$ Hz for individual residues in rI (**2**); $-27° < P_N < 46°$, $153° < P_S < 189°$, $30° < \Psi_m{}^N = \Psi_m{}^S < 35°$, rms < 0.15 Hz, $\Delta J_{max} < 0.30$ Hz for individual residues in flexrA (**3**); $-20° < P_N < 31°$, $143° < P_S < 165°$, $30° < \Psi_m{}^N = \Psi_m{}^S < 35°$, rms < 0.13 Hz, $\Delta J_{max} < 0.26$ Hz for individual residues in rA (**4**); $31° < P_N < 37°$, $153° < P_S < 196°$, $31° < \Psi_m{}^N = \Psi_m{}^S < 37°$, rms < 0.17 Hz, $\Delta J_{max} < 0.36$ Hz for individual residues in flexrG (**5**).

**Ab Initio Calculations.** Ab initio calculations on flexrG (**5**) were performed with the GAUSSIAN 98 software package using standard Gaussian 6-31G and 6-311G* basis sets.[14] The structure of flexrG (**5**) in (north, anti) conformation was first completely freely optimized at the HF/6-31G level. The conformational energy surface for flexrG (**5**) was constructed by constraining torsion angles $\chi$ [O4′−C1′−N9−C5] and $\phi$ [N9−C10−C4−N3] to fixed values and optimizing the rest of the molecule. The $\chi-\phi$ conformational space of flexrG (**5**) was scanned by incrementing both torsion angles in 30° steps from 0° to 360° which resulted in 144 energy points. Calculations were also performed on selected global and local energy minima geometries using the polarization continuum model (PCM) of Tomasi and co-workers.[15] The number of tessarae per sphere, which is a parameter of PCM calculation and defines the number of subdivisions of surface of each sphere into triangular tesserae,[14] was 80 in order to achieve convergence.

## Results

The conformational equilibria of fleximers flexrI (**1**), flexrA (**3**), and flexrG (**5**) and their natural analogues rI (**2**), rA (**4**), and rG (**6**) were evaluated with the use of $^1$H and 1D difference NOE NMR spectroscopy in $D_2O$ and DMSO-$d_6$ solutions. $^1$H NMR chemical shifts and $^3J_{HH}$ proton−proton coupling constants were measured in both solvents at four different temperatures between 298 and 358 K (see Tables 1S−3S in the Supporting Information). The temperature-dependent chemical shifts, $^3J_{HH}$ coupling constants, and NOE enhancements reflect time-averaged values of several rapidly interconverting conformers on NMR time scale in solution. Chemical shift changes in all studied compounds **1**−**6** at 10 mM concentration in DMSO-$d_6$ and in submillimolar concentration of **1**, **3**, and **5** in $D_2O$ showed linear dependence as a function of temperature. Such variation is typical for systems where intra- and intermolecular stacking interactions are not significant. The conformational equilibria of sugar moieties and along the C4′−C5′ bond (torsion angle $\gamma$) were assessed with the use of temperature-dependent $^3J_{1'2'}$, $^3J_{2'3'}$ and $^3J_{3'4'}$, and $^3J_{4'5'}$ and $^3J_{4'5''}$ proton−proton coupling constants, respectively (Tables 2S and 3S).


(7) Plavec, J.; Thibaudeau, C.; Chattopadhyaya, J. *Pure Appl. Chem.* **1996**, *68*, 2137−2144.
(8) Polak, M.; Mohar, B.; Kobe, J.; Plavec, J. *J. Am. Chem. Soc.* **1998**, *120*, 2508−2513.
(9) Thibaudeau, C.; Chattopadhyaya, J. *Stereoelectronic effects in nucleosides and nucleotides and their structural implications*; Uppsala University Press: Uppsala, Sweden, 1999.
(10) Plevnik, M.; Crnugelj, M.; Stimac, A.; Kobe, J.; Plavec, J. *J. Chem. Soc., Perkin Trans. 2* **2001**, 1433−1438.
(11) Thibaudeau, C.; Plavec, J.; Chattopadhyaya, J. *J. Org. Chem.* **1996**, *61*, 266−286.
(12) Haasnoot, C. A. G.; de Leeuw, F. A. A. M.; Altona, C. *Tetrahedron* **1980**, *36*, 2783−2792.
(13) Altona, C.; Francke, R.; de Haan, R.; Ippel, J. H.; Daalmans, G. J.; Westra Hoekzema, A. J. A.; van Wijk, J. *Magn. Reson. Chem.* **1994**, *32*, 670−678.
(14) Frisch, M. J.; Trucks, G. W.; Schlegel, H. B.; Scuseria, G. E.; Robb, M. A.; Cheeseman, J. R.; Zakrzewski, V. G.; Montgomery, J. A.; Stratmann, R. E.; Burant, J. C.; Dapprich, S.; Millam, J. M.; Daniels, A. D.; Kudin, K. N.; Strain, M. C.; Farkas, O.; Tomasi, J.; Barone, V.; Cossi, M.; Cammi, R.; Mennucci, B.; Pomelli, C.; Adamo, C.; Clifford, S.; Ochterski, J.; Petersson, G. A.; Ayala, P. Y.; Cui, Q.; Morokuma, K.; Malick, D. K.; Rabuck, A. D.; Raghavachari, K.; Foresman, J. B.; Cioslowski, J.; Ortiz, J. V.; Stefanov, B. B.; Liu, G.; Liashenko, A.; Piskorz, P.; Komaromi, I.; Gomperts, R.; Martin, R. L.; Fox, D. J.; Keith, T.; Al-Laham, M. A.; Peng, C. Y.; Nanayakkara, A.; Gonzalez, C.; Challacombe, M.; Gill, P. M. W.; Johnson, B. G.; Chen, W.; Wong, M. W.; Andres, J. L.; Head-Gordon, M.; Replogle, E. S.; Pople, J. A. *Gaussian 98*, revision A.5; Gaussian Inc.: Pittsburgh, PA, 1998.
(15) Barone, V.; Cossi, M.; Tomasi, J. *J. Chem. Phys.* **1997**, *107*, 3210−3221.

***Scheme 1.*** Structural Formulas of **1**−**6**

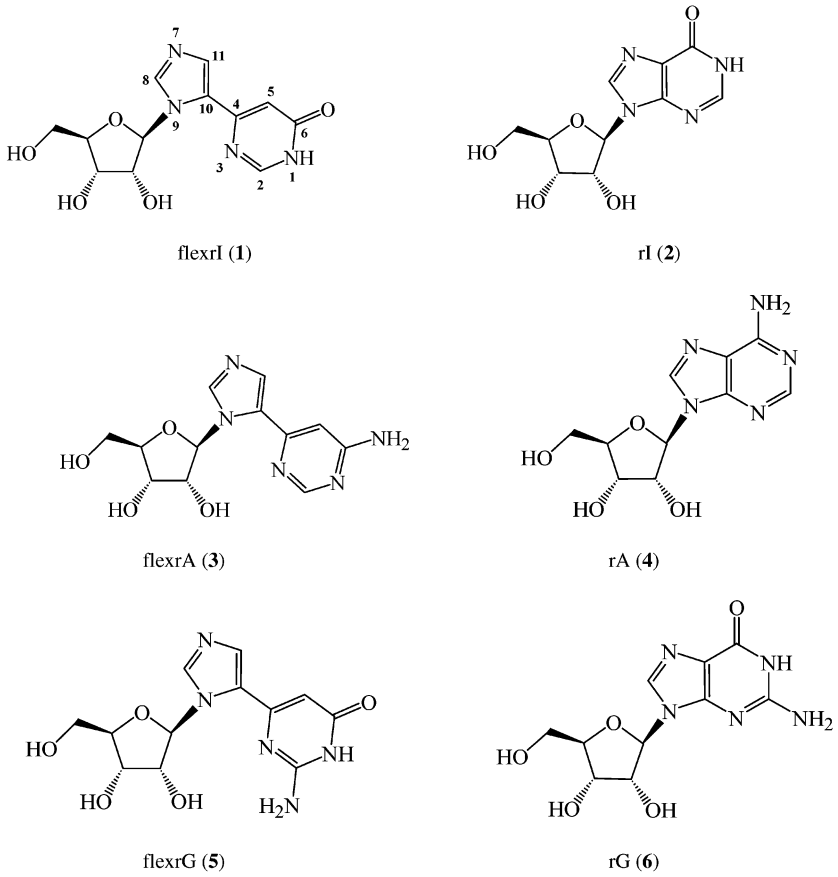


***Table 1.*** Pseudorotational Analysis and Population of $\gamma$ Rotamers in **1**−**6** at 298 K[a]

| compd | solvent | $P_N$ | $\Psi_m^N$ | $P_S$ | $\Psi_m^S$ | rms | $\Delta J^{max}$ | %*N* | %$\gamma^+$ | %$\gamma^-$ | %$\gamma^t$ |
|---|---|---|---|---|---|---|---|---|---|---|---|
| flexrI (**1**) | DMSO | 28 | 33 | 153 | 33 | 0.09 | 0.15 | 58 | 68 | 10 | 22 |
| | $D_2O$ | 28 | 34 | 152 | 34 | 0.08 | 0.21 | 60 | 60 | 8 | 33 |
| rI (**2**) | DMSO | 28 | 31 | 153 | 31 | 0.05 | 0.15 | 33 | 59 | 16 | 25 |
| flexrA (**3**) | DMSO | 28 | 33 | 156 | 33 | 0.04 | 0.08 | 55 | 68 | 9 | 23 |
| | $D_2O$ | 31 | 32 | 158 | 32 | 0.08 | 0.15 | 51 | 58 | 9 | 33 |
| rA (**4**) | DMSO | 39 | 31 | 160 | 31 | 0.03 | 0.07 | 28 | 67 | 12 | 21 |
| flexrG (**5**) | DMSO | 27 | 34 | 157 | 34 | 0.05 | 0.13 | 64 | 71 | 8 | 21 |
| | $D_2O$ | 36 | 34 | 169 | 34 | 0.06 | 0.13 | 62 | 60 | 8 | 33 |
| rG (**6**)[b] | DMSO | 36 | 32 | 156 | 32 | 0.04 | 0.08 | 33 | 52 | 24 | 24 |

[a] Phase angles of pseudorotation ($P_N$ and $P_S$) and maximum puckering amplitudes ($\Psi_m^N$ and $\Psi_m^S$) obtained with computer program PSEUROT are in degrees, rms errors and $\Delta J^{max}$ are in Hz, temperature is in K, and populations of N-type conformers and $\gamma$ rotamers are in %. [b] Taken from ref 10.

Equilibrium along the glycosidic bond (torsion angle $\chi$) was evaluated with the use of NOE enhancements.

**Conformational Equilibria of Ribofuranosyl Rings in 1−6 (Scheme 1).** The experimental $^3J_{HH}$ coupling constants which were acquired at four different temperatures were interpreted in terms of a two-state north (N) ⇄ south (S) pseudorotational equilibrium. The best fit between the experimental and calculated $^3J_{HH}$ coupling constants was found through iterative optimization of phase angles of pseudorotation and maximum puckering amplitudes of N ($P_N$ and $\Psi_m^N$) and S ($P_S$ and $\Psi_m^S$) pseudorotamers as well as their respective mole fractions (Table 1). Pseudorotational analysis of **1**−**6** revealed that N-type pseudorotamers of individual sugar moieties exhibit phase angles of pseudorotation ($P_N$) in the range from 27° to 39° (i.e., around C3′-*endo*−C4′-*exo* canonical form). The corresponding pseudorotamers in the south region of conformational space showed $P_S$ from 152° to 169° (ca. C2′-*endo* canonical form). The puckering amplitudes of both N and S pseudorotamers were found between 31° and 34° (Table 1). The comparison of pseudorotamer populations in Table 1 shows that the formal separation of the purine ring in **1**, **3**, and **5** with respect to their parent analogues **2**, **4**, and **6** leads to a significant increase in the population of N-type conformers for the former. Sugar moieties in natural ribonucleosides **2**, **4**, and **6** exhibited a 67−72% preference for S-type at 298 K, while N ⇄ S conformational equilibria in fleximer analogues **1**, **3**, and **5** were shifted toward the major N-type conformers (51−64% at 298 K). It is noteworthy that similar conformational preferences were found in $D_2O$ and DMSO-$d_6$ (Table 1).

Significant differences in temperature variation of N ⇄ S pseudorotational equilibria for **1**−**6** were found (Figure 1). To systematically evaluate variation of the population ratios for the fleximers and the parent nucleosides in Figure 1 in a more quantitative way, van't Hoff plots were employed. A van't Hoff analysis using populations of the N and S pseudorotamers at four different temperatures enabled calculation of the enthalpy and entropy contributions that drive the N ⇄ S equilibrium in **1**−**6** (Figure 2). The bar plots in Figure 2A show that the pseudorotational equilibrium is driven toward N-type conformers by enthalpy contributions for fleximers **1** and **5**, whereas it is weakly driven toward S for **3** in $D_2O$. The preferential drive of N ⇄ S equilibrium in **1**, **3**, and **5** toward N with respect to their natural counterparts **2**, **4**, and **6** is also observed in DMSO-$d_6$ (Figure 2B).

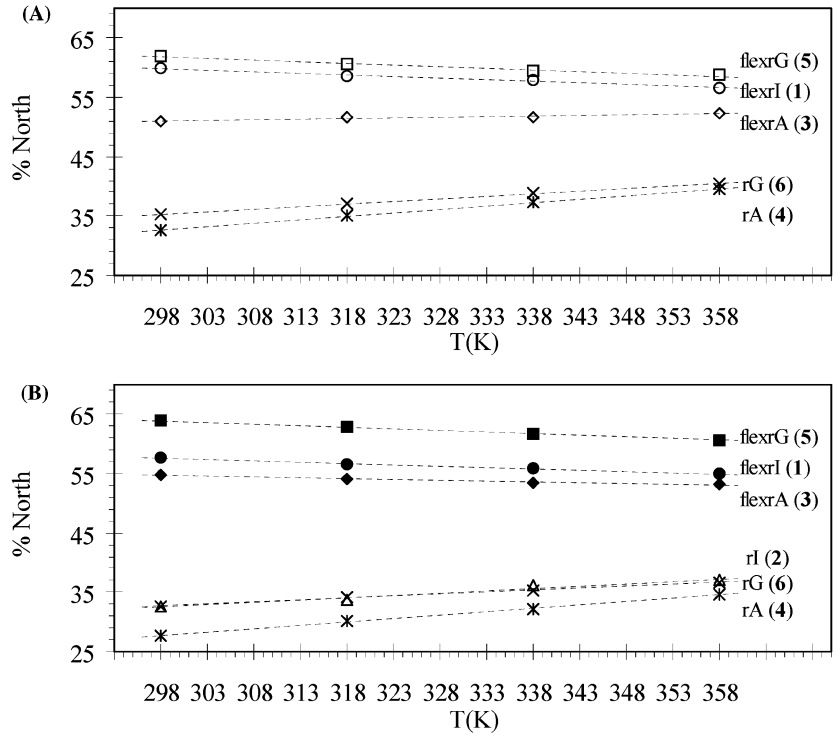


***Figure 1.*** Populations of north-type conformers in **1**−**6** in $D_2O$ (panel A) and in DMSO-$d_6$ (panel B).

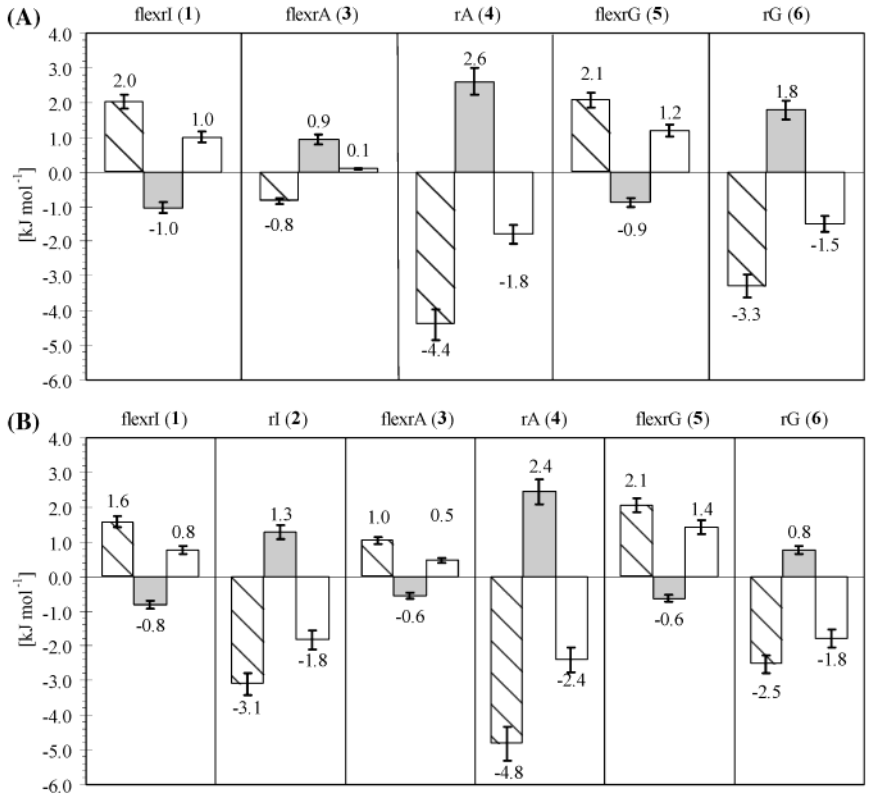


***Figure 2.*** Experimental thermodynamic parameters for N ⇄ S equilibrium in **1**−**6** at 298 K in $D_2O$ (panel A) and in DMSO-$d_6$ (panel B). The values of $\Delta H°$ and $\Delta S°$ were calculated from slopes and intercepts of van't Hoff plots according to the relation: $\ln(X_S/X_N) = -(\Delta H°/R)(1000/T) + \Delta S°/R$. $\Delta H°$ values are represented with dashed bars, $-T\Delta S°$ at 298 K are depicted with gray bars, and $\Delta G°$ values are depicted with white bars. The Pearson correlation coefficients of van't Hoff plots were −0.990 for **1**, 0.969 for **3**, and −0.996 for **5** in $D_2O$ and −0.995 for **1**, 0.985 for **2**, −0.984 for **3**, 0.999 for **4**, −0.999 for **5**, and −0.997 for **6** in DMSO-$d_6$. Error estimates are based on errors in the measurement of $^3J_{HH}$ coupling constants that were used to calculate the populations of N- and S-type pseudorotamers at individual temperatures.

**Conformation Equilibrium along the C4′−C5′ Bond (Torsion Angle $\gamma$).** Temperature-dependent $^3J_{4'5'}$ and $^3J_{4'5''}$ coupling constants were used to assess conformational equilibrium along C4′−C5′ bonds in **1**−**6** (i.e., torsion angle $\gamma$). Experimental coupling constants acquired at four different temperatures were interpreted in terms of a three-state $\gamma^+ \rightleftarrows \gamma^t$

***Table 2.*** 1D NOE Enhancements and Population of Syn Conformers in **1**−**6** at 298 K[a]

| compd | solvent | saturated | H2 | H5 | H8 | H11 | H1′ | H2′ | H3′ | H4′ | % syn |
|---|---|---|---|---|---|---|---|---|---|---|---|
| flexrI (**1**) | DMSO | H8 | | | | 0.8 | 1.1 | 7.9 | 2.3 | | 0−15 |
| | | H1′ | 1.6 | 8.3 | 0.9 | | | 2.9 | | 2.0 | |
| | | H5 | | | | 9.8 | 7.9 | | | | |
| | | H11 | | 10.1 | 0.4 | | | | | | |
| | $D_2O$ | H8 | | | | | 1.6 | 7.8 | 2.2 | | 0−15 |
| | | H1′ | 0.6 | 3.7 | 0.2 | | | 3.9 | 2.4 | | |
| | | H5 | | | | 1.3 | 4.2 | 0.6 | | | |
| | | H11 | | 7.5 | | | | | | | |
| rI (**2**) | DMSO | H8 | | | | | 7.6 | 6.8 | 1.2 | | 35−65 |
| | | H1′ | 0.7 | | 6.0 | | | 3.3 | | 2.4 | |
| flexrA (**3**) | DMSO | H8 | | | | 0.3 | 1.5 | 6.2 | 4.2 | | 0−15 |
| | | H1′ | 1.7 | 3.4 | 1.0 | | | 2.9 | 1.0 | 2.0 | |
| | | H5 | | | | 11.2 | 4.2 | | | | |
| | | H11 | | 11.2 | 0.2 | | 1.7 | | | | |
| | $D_2O$ | H8 | | | | | | 5.3 | 7.6 | 1.8 | 0 |
| | | H1′ | | 3.6 | | | | 1.1 | 3.6 | 2.23 | |
| | | H5 | | | | 4.6 | 4.8 | 1.7 | | | |
| | | H11 | | 8.0 | | | | | | | |
| rA (**4**) | DMSO | H8 | | | | | 9.9 | 4.9 | 0.7 | | 45−85 |
| | | H1′ | 0.7 | | 9.1 | | | 3.0 | 2.1 | | |
| flexrG (**5**) | DMSO | H8 | | | | 0.8 | 1.0 | 8.2 | *b* | | 10−15 |
| | | H1′ | | 8.1 | 1.1 | | | 2.9 | *b* | 1.6 | |
| | | H5 | | | | 13.5 | 6.0 | | | | |
| | | H11 | | 11.1 | 0.5 | | | | | | |
| | $D_2O$ | H8 | | | | | 1.5 | 7.0 | 2.5 | | 0−15 |
| | | H1′ | | 1.9 | | | | 2.8 | 0.4 | 2.8 | |
| | | H5 | | | | 1.0 | 2.8 | 0.3 | | | |
| | | H11 | | 5.6 | | | | | | | |
| rG (**6**) | DMSO | H8 | | | | | 5.9 | 7.0 | 1.1 | | 15−50 |
| | | H1′ | | | 4.2 | | | 2.6 | | 2.0 | |

[a] Values for enhancements are integrated areas under signals in % in comparison with the area under the signal for the saturated nucleus. The estimate of the population range of syn conformers is based on comparative analysis of H8 ↔ H1′ and H8 ↔ (H2′ + H3′) NOE enhancements.[17] [b] H3′ is nearly isochronous with H2′, and its NOE enhancements are included in values for H2′.

$\rightleftarrows \gamma^-$ equilibrium.[16] In all cases, $\gamma^+$ rotamers were preferred by 52% to 71% (see Tables 1 and 2S). The fleximers exhibited larger populations of $\gamma^+$ rotamers except in the case of the flexrA (**3**)/rA (**4**) pair where the differences were small. Lower $\gamma^+$ populations in natural nucleosides with respect to their fleximer counterparts are correlated with an increase in population of the $\gamma^-$ conformation for the former (Table 1).

**Conformation of Heterocyclic Aglycon (Torsion Angles $\chi$ and $\phi$).** 1D difference NOE experiments at 298 K were then performed to determine the preferred orientation along the glycosidic bond (i.e. syn $\rightleftarrows$ anti equilibrium) in **1**−**6**. Upon saturation of the H8 resonance, NOE enhancements were observed at H1′, H2′, and H3′ nuclei and used in the calculation of population of syn and anti conformations according to the equations: % syn = (100 × $\eta_{H1'}$)/11.3 and % anti = (100 × ($\eta_{H2'}$ + $\eta_{H3'}$)/9.6).[17] The results presented in Table 2 show a preference for syn conformation for the natural nucleosides. In contrast, their fleximer counterparts **1**, **3**, and **5** exhibited a lower preference for syn orientation with populations ranging from 0% to 15% in both $D_2O$ and DMSO-$d_6$ solutions (Table 2). The formal splitting of the purine into two rings apparently increases the steric bulk of the heterocyclic aglycon, which in turn shifts the equilibrium along the glycosidic bond in **1**, **3**, and **5** toward anti conformers.

(16) Haasnoot, C. A. G.; de Leeuw, F. A. A. M.; de Leeuw, H. P. M.; Altona, C. *Recl. Trav. Chim. Pays-Bas* **1979**, *98*, 576−577.
(17) Rosemeyer, H.; Toth, G.; Golankiewicz, B.; Kazimierczuk, Z.; Bourgeois, W.; Kretschmer, U.; Muth, H. P.; Seela, F. *J. Org. Chem.* **1990**, *55*, 5784−5790.

***Table 3.*** $T_1$ Relaxation Times for Proton Nuclei in **1**−**6** at 298 K[a]

| | flexrI (**1**) | | rI (**2**) | flexrA (**3**) | | rA (**4**) | flexrG (**5**) | | rG (**6**) |
|---|---|---|---|---|---|---|---|---|---|
| nucleus | DMSO | $D_2O$ | DMSO | DMSO | $D_2O$ | DMSO | DMSO | $D_2O$ | DMSO |
| H2 | 4.0 | 1.9 | 2.9 | 4.9 | 5.6 | 5.0 | | | |
| H5 | 1.6 | 1.8 | | 1.5 | 2.6 | | 1.5 | 1.1 | |
| H8 | 1.1 | 0.3 | 1.3 | 1.0 | 1.0 | 1.3 | 1.0 | 0.2 | 1.1 |
| H11 | 1.9 | 0.3 | | 1.4 | 1.3 | | 1.9 | 0.2 | |
| H1′ | 1.4 | 1.8 | 1.7 | 1.6 | 2.4 | 1.4 | 1.0 | 1.5 | 1.8 |
| H2′ | 0.7 | 1.3 | 0.8 | 0.7 | 1.8 | 0.8 | 0.5 | 0.9 | 0.7 |
| H3′ | 0.8 | 1.3 | 0.8 | 0.8 | 1.6 | 0.8 | 0.5 | 1.0 | 0.8 |
| H4′ | 0.9 | 1.5 | 1.0 | 0.9 | 1.4 | 1.0 | 0.7 | 1.3 | 1.0 |
| H5′ | 0.5 | 0.5 | 0.3 | HOD | 0.6 | 0.3 | 0.3 | 0.5 | 0.3 |
| H5″ | 0.3 | 0.5 | 0.3 | 0.3 | 0.6 | 0.3 | 0.3 | 0.5 | 0.3 |

[a] $T_1$ relaxation times (in s) have been calculated by fitting the experimentally determined signal intensities obtained by inversion recovery experiments. Standard deviations in $T_1$ values were below 30 ms, except for H1′ in **5** and H5′ in **1** recorded in DMSO-$d_6$ and H2, H2′, and H4′ in **3** in $D_2O$, where they were below 75 ms.

The relative orientation of the imidazole and pyrimidine rings is defined by the use of torsion angle $\phi$ [N9−C10−C4−N3]. Almost coplanar alignment of both imidazole and pyrimidine moieties ($\phi \approx 0°$) in flexrG (**5**), where the $NH_2$ group on the latter is pointing toward the sugar moiety, is supported by experimental NOE data and has also been found by ab initio calculations to be energetically preferred (vide infra). Specifically, NOE enhancements at H5 upon saturation of H11 in **1**, **3**, and **5** in $D_2O$ range from 5.6% to 8.0% (Table 2) which corroborates their short internuclear distance and high population of conformers with a coplanar imidazole and pyrimidine ring orientation. Most heterocyclic proton atoms including H5 in particular exhibit considerably smaller magnitudes of NOE enhancements in $D_2O$ compared to DMSO-$d_6$, which indicates the effect of hydration of nearby hydrophilic groups and proton exchange of imino and amino groups on dipole−dipole interactions. Some minor conformational readjustments in $\phi$ as well as change in rotamer populations along C4−C10 bonds in **1**, **3**, and **5** are also expected to occur in the two solvents.

**$^1$H $T_1$ Relaxation Times.** $^1$H spin−lattice relaxation time ($T_1$) measurements were then performed to examine possible changes in the relaxation properties of modified nucleosides **1**, **3**, and **5** due to the increased flexibility along the C−C bond that resides within the heterocyclic moiety. Randomly fluctuating fields experienced by the nucleus are caused by tumbling and other motions of the nucleus itself and other nuclei in the molecule or in solution and are reflected in longitudinal relaxation of the studied proton. $T_1$ values of heterocyclic and sugar proton resonances (Table 3) are sensitive to conformational changes of the sugar ring and the orientation along the glycosidic bond.[18] Qualitative analysis of $T_1$ values is in agreement with the observation of higher populations for anti and N-type sugar conformers in fleximers **1**, **3**, and **5** as compared to the natural nucleosides **2**, **4**, and **6**, respectively. Namely, noticeable differences of up to 1.1 s in $T_1$ relaxation times were observed for H2, H8, and H1′ in the fleximers in comparison to their natural counterparts (Table 3). This suggests increased dynamics of nuclei in this part of the molecule and is in agreement with reorientation along the $\chi$ torsion angle supported by the NOE data. It is interesting to note that there is a considerable drop in $T_1$ values in $D_2O$ in comparison to DMSO-$d_6$. The decrease is larger for protons of pyrimidine and imidazole moieties than for sugar rings.

(18) Shibata, S. *Magn. Reson. Chem.* **1992**, *30*, 371−376.

***Table 4.*** Energy Minima Conformations of flexrG (**5**) Obtained by Ab Initio Optimizations at the HF/6-31G Level[a]

| conformer | $\chi$ | $\phi$ | $P_N$ | $\Psi_m^N$ | $E_{rel}$ (HF) | $E_{rel}$ (PCM, DMSO) | $E_{rel}$ (PCM, water) |
|---|---|---|---|---|---|---|---|
| (anti, sp) | −162 | −12 | 27 | 38 | 0.0 | 0.0 | 0.0 |
| (anti, ap) | −162 | 173 | 27 | 39 | 17.8 | 19.5 | 7.1 |
| (syn, sc) | 46 | 44 | 62 | 38 | 35.6 | 35.2 | 26.0 |
| (syn, sc) | 84 | −43 | 56 | 37 | 46.9 | 44.7 | 37.7 |

[a] Values for torsion angles $\chi$ [O4′−C1′−N9−C5] and $\phi$ [N9−C10−C4−N3], phase angle of pseudorotation ($P_N$), and puckering amplitude ($\Psi_m^N$) are in degrees; $E_{rel}$ is in kJ mol$^{-1}$. The lowest HF energies in vacuo (−1109.210 89 au) and in PCM calculations with DMSO (−1109.238 85 au) and with aqueous (−1109.267 57 au) environments were used as arbitrary reference points. The single-point HF/6-311G* relative energies in vacuo for the conformers optimized at the HF/6-31G level were 0.0 (−1109.937 76 au), 17.5, 23.0, and 31.1 kJ mol$^{-1}$.

**Ab Initio Calculations.** We then performed a set of ab initio calculations on flexrG (**5**) at the HF/6-31G level in order to construct a $\chi-\phi$ potential energy surface. Unrestricted optimization at the HF/6-31G level with the N-type sugar conformation ($P = 11°$, $\Psi_m = 38°$) and nucleobase in anti conformation ($\chi = 180°$, $\phi = 0°$) of flexrG (**5**) was performed at the initial stage of simulations. This optimized structure ($P = 27°$, $\Psi_m = 38°$, $\chi = -162°$, $\phi = -12°$, Table 4) was subsequently used in the construction of the $\chi-\phi$ potential energy surface. In calculating the potential energy surface points, torsion angles $\chi$ [O4′−C1′−N9−C5] and $\phi$ [N9−C10−C4−N3] were incremented in 30° steps from 0° to 360° and fixed, while all other conformational degrees of freedom were freely optimized. The energies of the resulting 144 structures were used to construct a 3D surface plot (Figure 3). The potential energy surface exhibits a global minimum characterized by $\chi$ in the anti range ($\chi \approx 180°$) and $\phi$ in the sp range ($\phi \approx 0°$) (Figure 3). The conformational reorientation of the nucleobase from anti to syn conformation with respect to the sugar moiety is energetically demanding (barrier ≈ 70 kJ mol$^{-1}$). The rotation along torsion angle $\phi$ exhibits a slightly lower energy barrier of up to 50 kJ mol$^{-1}$ (Figure 3). Unrestricted energy optimizations were performed in the above energy minima, which resulted in two conformers in the anti region and two in the syn region of conformational space (Table 4). The two lowest energy structures are presented in Figure 4. Several attempts to calculate relative energies in (syn, sp) and (syn, ap) conformational regions for flexrG (**5**) consistently resulted in the above energy minima, which is probably due to unfavorable steric interactions. Additional energy calculations were performed on freely optimized structures using the PCM model to evaluate effects of solvatation. The energy difference between the two lowest energy conformers was comparable in vacuo and in DMSO ($\Delta\Delta = 1.7$ kJ mol$^{-1}$). The relative stabilization of the *anti*-sp over *anti*-ap conformer was considerably smaller in an aqueous environment (Table 4).

## Discussion

It is well established that the puckering of sugar moieties in nucleosides and nucleotides and thermodynamics of N ⇄ S pseudorotational equilibrium are governed by the competing steric, gauche, and anomeric effects.[6,8] The N ⇄ S pseudorotational equilibrium in individual nucleosides **1**−**6** is driven toward N by the anomeric effect of a heterocyclic nucleobase and by the gauche effect of [O4′−C1′−C2′−O2′] fragment. These effects, however, are opposed by the gauche effects of [O4′−C4′−C3′−O3′] and [N9−C1′−C2′−O2′] fragments that drive pseudorotational equilibrium toward S-type conformers. The anomeric effect, which drives the N ⇄ S equilibrium toward N-type conformers, is strengthened when the electron-accepting ability of the nucleobase increases as exemplified by protonation or upon interaction with $M^{2+}$ ions.[11,19−22] On the other hand, the steric effect of the nucleobase drives the N ⇄ S equilibrium through the preference of bulky substituents to adopt a pseudoequatorial orientation and thus favors an S-type conformation.

Our pseudorotational analysis has shown that fleximers **1**, **3**, and **5** are involved in a conformational equilibrium between puckered north (around C3′-*endo*−C4′-*exo* canonical form) and south forms (around C2′-*endo* canonical form) with comparable $P$ and $\Psi_m$ values as found in their natural counterparts **2**, **4**, and **6**. Considerably higher populations of N-type conformers were observed for fleximers **1**, **3**, and **5**. The increase in the populations of N-type conformers varies from 25 unit % in the case of the flexrI (**1**)/rI (**2**) pair, 27 unit % in the case of the flexrA (**3**)/rA (**4**) pair, to as high as 31 unit % for the flexrG (**5**)/rG (**6**) pair in DMSO-$d_6$ at 298 K. The population difference in $D_2O$ is reduced to 18 unit % in the case of the flexrA (**3**)/rA (**4**) pair and 27 unit % for the flexrG (**5**)/rG (**6**) pair. These experimental observations can be rationalized by considering the changes in the three competing factors and their related stereoelectronic effects upon substitution of the natural heterocyclic nucleobase with a flexible analogue: (i) the anomeric effect of the nucleobase drives the N ⇄ S pseudorotation equilibrium toward N-type conformers; (ii) the steric effect of the nucleobase and (iii) the gauche effect of the [N9−C1′−C2′−O2′] fragment both drive the N ⇄ S pseudorotation equilibrium in **1**−**6** toward S-type conformers.

Unfortunately, the relative strengths of the anomeric and gauche effects of the [N9−C1′−C2′−O2′] fragment in fleximer nucleosides **1**, **3**, and **5** cannot be measured directly and dissected through comparative analysis of thermodynamics of their N ⇄ S equilibrium. It is known, however, that substitution of guanine or adenine by an imidazole ring in 2′-deoxyribonucleosides shifts the N ⇄ S pseudorotation equilibrium toward N-type conformers by only 2 and 4 percentage points at 298 K, respectively.[9] This clearly demonstrates that the substitution of the bicyclic purine nucleobase with an imidazole ring induces a small increase in the strength of the anomeric effect and/or a small decrease in steric bulk. A pairwise comparison between 2′-deoxy- and ribonucleosides that elaborates the effect of 2′-OH group interactions with adenine and guanine nucleobases also showed only a 2 and 3 percentage point increase in the populations of N-type conformers for guanosine and adenosine, respectively, with regards to their 2′-deoxy counterparts.[9] The introduction of the 2′-OH group that is involved in two gauche effects of [N9−C1′−C2′−O2′] and [O4′−C1′−C2′−O2′] fragments which oppose each other in the drive of N ⇄ S equilibrium therefore results in only a small effect. If the gauche effect of the [O4′−C1′−C2′−O2′] fragment is comparable in fleximers **1**, **3**, and **5** and in their natural analogues **2**, **4**, and **6**, respectively, we could expect only a small shift of a few percent

(19) Polak, M.; Plavec, J. *Nucleosides Nucleotides* **1998**, *17*, 2011−2020.
(20) Polak, M.; Plavec, J.; Trifonova, A.; Foldesi, A.; Chattopadhyaya, J. *J. Chem. Soc., Perkin Trans. 1* **1999**, 2835−2843.
(21) Polak, M.; Plavec, J. *Nucleosides Nucleotides* **1999**, *18*, 1109−1112.
(22) Polak, M.; Plavec, J. *Eur. J. Inorg. Chem.* **1999**, 547−555.

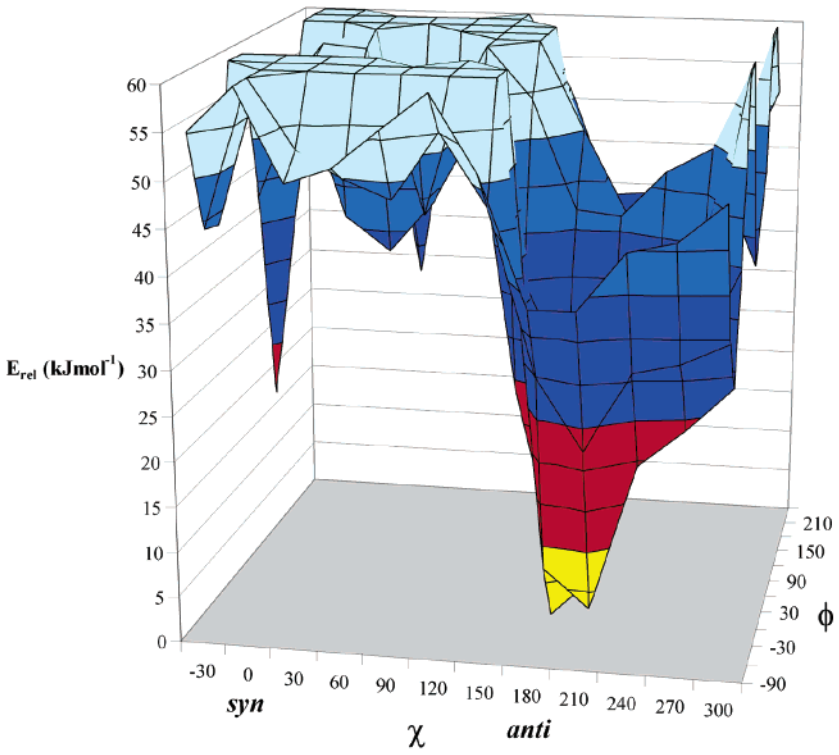


***Figure 3.*** Ab initio HF/6-31G potential energy surface of flexrG (**5**) showing global minimum for the conformations with a heterocyclic nucleobase in the (anti, sp*)* region ($\chi \approx 180°$, $\phi \approx 0°$). Other local minima are in the following four conformational regions: (anti, ap) region ($\chi \approx 180°$, $\phi \approx 180°$, $E_{rel} = 19.3$ kJ mol$^{-1}$), (syn, sc) region ($\chi \approx 60°$, $\phi \approx 60°$, $E_{rel} = 39.9$ kJ mol$^{-1}$), (syn, ac) region ($\chi \approx 60°$, $\phi \approx 150°$, $E_{rel} = 35.3$ kJ mol$^{-1}$), and (syn, sc) region ($\chi \approx -30°$, $\phi \approx 90°$, $E_{rel} = 26.4$ kJ mol$^{-1}$).

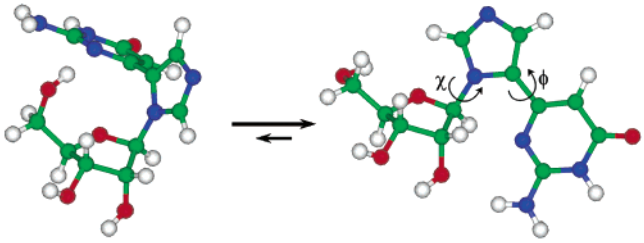


***Figure 4.*** Conformational equilibrium between two lowest energy conformers of flexrG (**5**) as obtained from ab initio potential energy surface at the HF/6-31G level. The left side molecule exhibits (syn, sc) conformation ($\chi \approx -30°$, $\phi \approx 90°$, $E_{rel} = 26.4$ kJ mol$^{-1}$), while the right side structure is a global minimum and is characterized by (anti, sp*)* conformation ($\chi \approx 180°$, $\phi \approx 0°$, $E_{rel} = 0.0$ kJ mol$^{-1}$) of the nucleobase.

toward N-type conformers in fleximer nucleosides in comparison to the natural ones due to the change of the nucleobase.

Modification of the nucleobases from natural inosine, adenosine and guanosine into their corresponding fleximer analogues leads to increased populations of anti conformation along glycosidic bond. It is reasonable then to assume that the steric effect is increased, which indicates that the fleximer nucleobases drive N $\rightleftarrows$ S pseudorotation equilibrium toward S-type conformers more efficiently than the parent natural nucleobases. We have, however, observed considerable stabilization of N-type conformers for fleximer analogues **1**, **3**, and **5**. The formal splitting of the bicyclic purine ring into its five-membered imidazole and adjacent six-membered pyrimidine rings imposes some additional effects on the pentofuranose ring conformation due to the additional degrees of freedom (e.g., $\phi$). One possible explanation is the formation of a hydrogen bond between the $NH_2$ group on the pyrimidine ring and the 2′-OH of the pentofuranose moiety. Comparison of molecular models obtained by ab initio calculations and supported by 1D difference NOE experiments ($\chi \approx 180°$ and $\phi \approx 0°$) demonstrates that the distances between O2′ and hydrogen atoms of the $NH_2$ group are ca. 2.2 Å for both N- and S-type conformers of flexrG (**5**). Formation of such a hydrogen bond requires anti conformation ($\chi \approx 180°$) and nearly coplanar pyrimidine and imidazole rings ($\phi \approx 0°$) but does not favor N- over S-type sugar conformation (Figure 4). The hydrogen bond O2′- - -HN could therefore represent a conformational lock that stabilizes anti conformation in flexrG (**5**). The rotation across the C4−C10 bond in flexrA (**3**) would hypothetically lead to formation of such a hydrogen bond between its O2′ and C6−$NH_2$ group. Our ab initio calculations, however, clearly showed that such a conformer ($\phi = 170°$, $\chi = -160°$) was energetically unfavored by 12.4 kJ mol$^{-1}$ at the HF/6-31G level of theory over the rotamer of flexrA (**3**) where its pyrimidine adopted a conformation with the amino group turned away from the ribose moiety ($\phi = -14°$, $\chi = -161°$). It is noteworthy that results of our ab initio calculations are in full agreement with our NMR data. Fleximer nucleosides described in this work show resemblance to ribavirin, which exhibits a broad spectrum of antiviral activity.[23] Several studies have shown that the pseudo base (1,2,4-triazole-3-carboxamide) of ribavirin is capable of base-pairing equivalently with cytidine and uridine as long as rotation of the carboxamide moiety is not restricted.[23−26] An earlier NMR

(23) Witkowski, J. T.; Robins, R. K.; Khare, G. P.; Sidwell, R. W. *J. Med. Chem.* **1973**, *16*, 935−937.
(24) Crotty, S.; Maag, D.; Arnold, J. J.; Zhong, W. D.; Lau, J. Y. N.; Hong, Z.; Andino, R.; Cameron, C. E. *Nat. Med.* **2000**, *6*, 1375−1379.
(25) Ulrich, S. M.; Sallee, N. A.; Shokat, K. M. *Bioorg. Med. Chem. Lett.* **2002**, *12*, 3223−3227.
(26) Wu, J. Z.; Lin, C. C.; Hong, Z. *J. Antimicrob. Chemother.* **2003**, *52*, 543−546.

study[27] showed that ribavirin is involved in N ⇄ S equilibrium with essentially equal contributions of the two pseudorotamers. North over south conformational preferences in **1**, **3**, and **5** could not be interpreted without involving interactions of the $\pi$-systems of imidazole and pyrimidine moieties. Coplanar arrangement of the imidazole and pyrimidine rings might lead to conjugation of their $\pi$-electron clouds in the fleximer nucleobases and thus strongly strengthen the anomeric effects. Electron delocalization from the imidazole part of the molecule is consistent with a stronger anomeric effect and induces a large shift of the N ⇄ S pseudorotation equilibrium toward N-type conformers which has been experimentally observed for **1**, **3**, and **5**.

It was originally proposed[5] that the fleximer nucleobases could adopt a syn conformation to better accommodate the active site on the SAHase enzyme. The NMR study presented here on the unrestricted fleximer nucleosides **1**, **3**, and **5** in solution in the absence of enzyme showed a strong preference of the syn ⇄ anti equilibrium for anti conformers. This result is in agreement with the potential energy surface for flexrG (**5**) at the HF/6-31G level in vacuo (Figure 3) which showed a global minimum in the (anti, sp) region ($\chi = -162°$, $\phi = -12°$). The pyrimidine and imidazole moieties were also found to exist preferentially in a coplanar arrangement. Our studies at the HF/6-31G level indicate that the syn conformation has a considerably higher energy.

In conclusion, the experimental NMR and ab initio calculations presented herein demonstrate a great increase in populations of N-type conformers as a result of the modification of the heterocyclic nucleobase from the natural purine to the fleximer analogues. We have found that the increased steric bulk of the fleximer nucleobase and the possible formation of a hydrogen bond between the $NH_2$ group on the pyrimidine ring and the 2′-OH induced a shift toward higher populations of anti conformation in the fleximers. No significant redistribution along the C4′−C5′ bond was detected which reveals that no major disruption on that portion of the sugar ring takes place upon formal separation of the purine moiety. The ab initio energy surface for flexrG (**5**) exhibited energy minima in the syn region, which could support the possible stabilization of the syn conformation in the binding site of the SAHase enzyme. Taken together, this evidence clearly illustrates that the interplay of stereoelectronic effects, the relative flexibility of the nucleobase, combined with the potential for increased conjugation effects for the nucleobase, which in turn strengthens the anomeric effect, all play crucial roles in predicting conformations for flexible molecules. Given the elusive nature of tertiary enzyme structure, gaining a better understanding of these conformational effects will further aide in the design of flexible bioprobes to help with the structural elucidation of ligand binding sites in biologically significant enzymatic systems.

**Acknowledgment.** We thank the Ministry of Education, Science and Sport of Republic of Slovenia (Grant Nos. J1-3309-0104 and P1-0242) and European Commission (ICA1-CT-2000-70034) for financial support.

**Supporting Information Available:** Tables containing experimental NMR chemical shifts and $J_{HH}$ coupling constants. This material is available free of charge via the Internet at http://pubs.acs.org.

JA0498078

(27) Dea, P.; Schweizer, M. P.; Kreishman, G. P. *Biochemistry* **1974**, *13*, 1862−1867.